Simulation-based study of the Implementation of Bio-Inspired Riblets in Supersonic Nozzles

Aakash Ghosh[a], Shashwat Patnaik[b], Raj Kumar Singh[c]

[a]*Department of Aerospace Engineering, Delft University of Technology, Delft, The Netherlands 2629 HS*
[b]*Department of Aerospace Engineering, University of Michigan, Ann Arbour, USA MI 48109*
[c]*Department of Mechanical Engineering, Delhi Technological University. Rohini, New Delhi, India 110042*

Abstract

The ever-increasing demand for high-performance rocket propulsion systems has led engineers to increase the Nozzle's expansion ratio. However, it has led to further challenges such as flow separation and asymmetric forces, which have limited the Nozzle's performance and other engine components. This paper aims to develop a simulation framework to test the effects and viability of ribletted surfaces on nozzles. This study presents a compressible-Reynolds-Averaged Navier Stokes simulation of a convergent-divergent nozzle fitted with riblets. Furthermore, the basic sawtooth and the U-shaped riblets are tested and compared while keeping the height-by-spacing ratio constant. Analysis of the contours suggests the production of secondary flows around the riblets and is seen to help delay the boundary layer separation. The wall shear stress contours are also studied, and it is observed that the riblets help localize high stress to their tips. Comparison between the kinetic energy values of the sawtooth and the U-shaped riblets show that the U-shaped riblets produce secondary flows, which are nearly twice as strong as the sawtooth riblets.

Keywords: Biomimetics; Computational Fluid Dynamics; Riblets; Supersonic Nozzle; Secondary Flows

1. Introduction

The most critical component of the rocket's propulsion system is the nozzle. The aerodynamic design of the nozzle, such as its geometrical shape and the expansion ratio, are critical factors governing the performance of the rocket's propulsion system. Hence, the efficiency of the nozzle is limited by the expansion ratio of the nozzle. It is desirable to have a large expansion ratio to generate an enormous thrust. However, a large expansion ratio becomes challenging at low altitude levels, especially at rocket start-up or when the nozzle's flow is overexpanded due to the flow getting separated. Many unconventional mechanisms and features are evolved in nature to maximize the speed or maneuverability of animals in water or air. Many scientists have adapted these evolutionary changes present in nature to improve current technology. Sharks are a great example, where through evolution, they have developed patterned surface roughness allowing them to decrease the overall drag, making them swim faster.

The aggressive expansion ratio leads to flow being separated at the nozzle wall itself. It is typically caused by a shock wave as the flow is accelerated while the pressure drops precipitously. Due to the pressure drop, the flow jumps through the shock wave to equilibrate to the atmospheric pressure. When this occurs, the shock wave's position is unsteady and frequently asymmetric, creating various dynamic loads on the nozzle. The asymmetric and unsteady nature of the flow leads to these lateral forces, also known as side loads [1]. These forces can create numerous challenges during the rocket's stabilization at lower altitudes.

Fig 1. shows that the shock wave is asymmetric, forming a large separation region on one side and smaller on the other. This makes the shock wave unstable, oscillating forward and back spontaneously [2]. The ever-increasing demand for higher performance rocket propulsion systems has led to the development of nozzles having larger expansion ratio to sustain high amount of thrust, but it has magnified the problem of flow separation and lateral forces, which are present during a majority part of the rocket’s ascent.

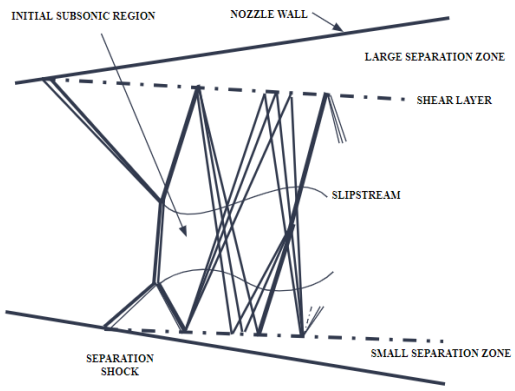

Fig. 1. Shockwave Diagram

Researchers have proposed numerous solutions where the Nozzle may adapt the contour while in flight to adapt to the ambient and chamber pressures changes. Nevertheless, there has not been a successful implementation of such a system due to its weight and mechanical complexity [3, 4]. Mimicking natural mechanisms into various industries has become an effective technique to tackle numerous challenges related to current technologies. One such aerodynamic device is riblets which are bio-inspired surface patterns seen on sharks. Riblets induce secondary flow due to their geometric features resulting in lower drag, making it possible for sharks to achieve such high speeds. They are proven to reduce momentum losses, thus delaying the boundary layer separation [5]. Riblets have already been used in aerospace industry in both subsonic and supersonic flow [5]. These bio-inspired riblets can be embedded inside the rocket nozzle's surface to delay the boundary layer separation, reducing the side-load.

1.1 Literature Review

The research conducted by Michael J. Walsh of NASA Langley Research Centre on turbulent boundary layer flow over longitudinally grooved surfaces at low speed. He observed that the introduction of riblets could produce consistent net drag reductions as significant as 8 percent [6]. Similar results were recorded under supersonic flow conditions. The experimental study performed by K. Tsunoda explores the improvement in the performance of a Supersonic Nozzle by embedding riblets along the surface of the nozzle. It utilized Pitot-tube to obtain the Mach number distributions concluded that the separation point moved downstream and the size of the separation region became small when using riblets [7]. Additionally, the research done by D. B. Goldstein found that riblets in a channel bounding fully developed turbulent flow can produce a pattern of secondary mean flows consisting of matched pairs of streamwise vortices [8]. He further suggested that these secondary flows are strongly linked with the decrease in drag experienced.

Although extensive research has been done to prove the effectiveness of Riblets in delaying the boundary layer separation, only a handful of papers evaluate the effectiveness of Riblets in improving the flow characteristics of the nozzle. The research conducted by Tsunoda et al. (2000) evaluates improvement of the nozzle with riblets but fails to correlate with rocket nozzle. Several studies have shown that interaction between the boundary layer and shock wave formed inside the nozzle can lead to adverse effects. Such as the paper by Stark et al. (2013) considers a simple model and evaluates the various mechanisms leading to the interaction and its consequential effects on the nozzle's performance [2]. This paper evaluates the feasibility of Riblets to delay the boundary layer separation in rocket nozzles to decrease dynamic loads (side-load). Moreover, the effectiveness of different shapes of riblets is investigated and compared. Lastly, this paper aims to develop a sustainable CFD framework to study the effect of such surface patterns in nozzles. The use of RANS coupled with a fine mesh facilitates a low computational load model, significantly reducing costs for running experimental investigations and further opens avenues for performing design optimization of the riblets.

1.2 Interactions between Shock-Wave and Boundary Layer

When an adverse pressure gradient interacts with a supersonic flow, the flow will adapt to the higher-pressure

level through a complex shock wave system [1]. Hence, the turbulent boundary layer is unable to sustain the adverse pressure gradient imposed by the outer flow, leading to flow getting separated from the nozzle's wall. The phenomenon of flow separation in a rocket's nozzle involves complex interactions between the shock-wave and the boundary-layer in a supersonic flow [2].

A similar phenomenon is observed when a nozzle's condition is overexpanded. When a nozzle is overexpanded, the oblique shock is formed to recompress the pressure to the backpressure of the exhaust system. At overexpanded flow conditions in the Nozzle, the ratio $n = P_{e,vac} / P_a < 1$ (n is used to define flow condition, where n =1 is ideal condition and n > 1 indicates under expansion) [8]. The instant n is less than 1; an adverse pressure gradient is formed causing formation of an oblique shock at the nozzle outlet. If the n is then reduced further, the boundary layer is unable to withstand the adverse pressure gradient, leading to separation from the wall [2]. The boundary layer cannot withstand the significant increase in the pressure caused due to the intense shock formed at the nozzle outlet [1]. Thus, consequently, the shock begins to move along the Nozzle's wall while remaining in oblique form [9]. The nozzle flow separation leads to the formation of difference in the pressure between the inner and outer nozzle surface as shown in Fig. 1. The asymmetric nature of the separation creates a "side-load" forces. The interaction between the shock wave and boundary layer can cause:

- Increase in frictional drag, mainly if the Nozzle is long.
- It may increase entropy production (because of shock wave interaction) [1].
- Affects the stabilization of the rocket at lower altitudes because of slide-loads.
- The nozzle and other engine components may get damage if the side loads are excessive.
- Overall nozzle efficiency decreases and specific Impulse decreases [1].

1.3 Riblets on Rocket Nozzle

In order to adapt and survive the ever-changing environment of Earth, evolution is a crucial component. It is a series of biological optimizations allowing several different biological beings to adapt to various new challenges. One of these evolutions was observed on sharks. Their evolutionary feature of patterned surface roughness has allowed them to alter fluid flow around the body to reduce the overall drag [10].

Fig. 2 depicts the microscopic view of the Mako shark's skin. These subspecies are well known for their fast speeds. These surface patterns were also observed in the beaks of skimmer birds, making them more aerodynamic in nature. Evolution in this manner has been occurring for millions of years [10]. Biomimicry is the process of imitating biological mechanisms in artificial mechanisms [11]. Several different areas of engineering have adopted biomimetics to improve their current designs.

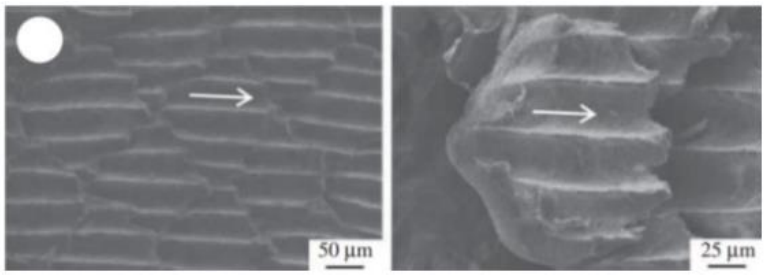

Fig. 2. Riblets on a Mako Shark (Martin & Bhushan, 2016) [13]

A riblet a longitudinally micro-grooved surface used as a passive drag-reduction techniques first by NASA [11]. The systematic study was first initiated to reduce airlines' fuel costs by NASA Langley Research Centers [6]. Riblets have always been an area of interest in reducing aerodynamic drag over an aircraft. A critical feature of riblets is to produce secondary flows.

Secondary flows are sub-categorized into two types: Prandtl's First Kind and Prandtl's Second Kind.

The first kind is created by 'skew induced' secondary flow. In contrast, the second kind is a product of both skew and stress. Prandtl's second kind can only be formed under turbulent conditions [11]. For riblets, it is not easy to highlight the type of secondary flow being produced. It is commonly considered to induce secondary flows of a third

kind [5], primarily driven by viscous forces. Several experimental studies Walsh (1983) [6], Lee & Lee (2001) [12] as well as numerical and simulation-based studies Goldstein, 1998 [8]; researchers further demonstrated that the introduction of riblets concentrates the wall shear stress onto the tip of the riblets, therefore, decreasing the total area over which the stress acts. The experimental study on flat plates by Lee & Lee (2001) also noticed that the turbulent kinetic velocity and RMS velocity fluctuations are more significant on ribletted surfaces [12]. Larger velocity and kinetic energy cause the boundary layer separation to be delayed. An experimental study by Gaudet demonstrated by the direct measurement of shear stress that similar benefits were achieved by using riblets at supersonic speeds.

2. Methodology

This study uses a systematic approach to develop the CFD framework. The study by Tsunoda et al. (2000) gives an experimental study of the use of riblets on a Convergent-Divergent Nozzle, which is used to validate this study's model. Their study tested two riblet geometries; both have an identical wavelength but have different heights; however, a slightly better flow behavior was noticed in the smaller height. They also use multiple pressure ratios, and for this study, a pressure ratio of 0.1 is used. The experimental setup used in the study uses a 400 mm long nozzle setup with a width of 30 mm. Though the length of the nozzle was kept the same, the width was decreased to reduce the computational load [7]. The geometry and the boundary conditions are taken from this study, and the results are then compared against their experimental outputs.

2.1 Mesh Development

The meshing of the geometry is an essential part of developing the framework. The mesh was produced using the OpenFOAM in-built functions 'blockMesh' and 'snappyHexMesh'. The base nozzle geometry and mesh were created using the blockMesh feature. A relatively fine mesh is developed in order to reuse the same mesh for snapping when using riblets. The base mesh consists of 2,016,000 hexahedral cells and takes 6 seconds to form.

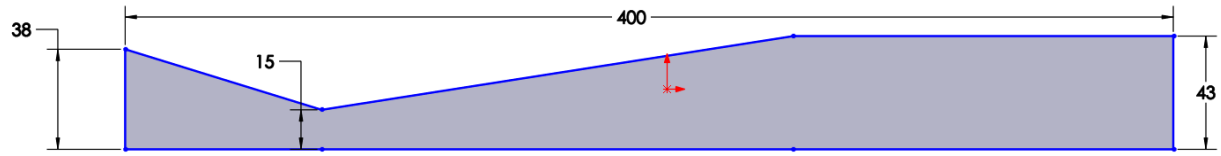

Fig. 3. Nozzle Dimensions (in mm)

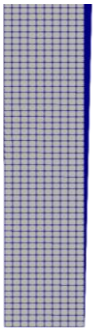
Fig. 4. Base Mesh (Front View)

The riblet CAD was created using SolidWorks and expired as STL files which were used for snapping. The height (h) of the riblets is taken as 0.022mm and the spacing (s) is 0.050mm based on study [9]. Snapping was done using a SnappyHexMesh command, which is a Boolean operation used to remove specific mesh cells and refine the mesh at particular points. The SnappyHexMesh feature develops a hexahedral mesh domain, wherein a geometric cell is made of edges, quadrilaterals and hexahedra such that each node is bound by at least 3 edges. Given the heavy CAD model and high transition between zones of refinement, the overall mesh generation for one case took approximately 1,500 seconds.

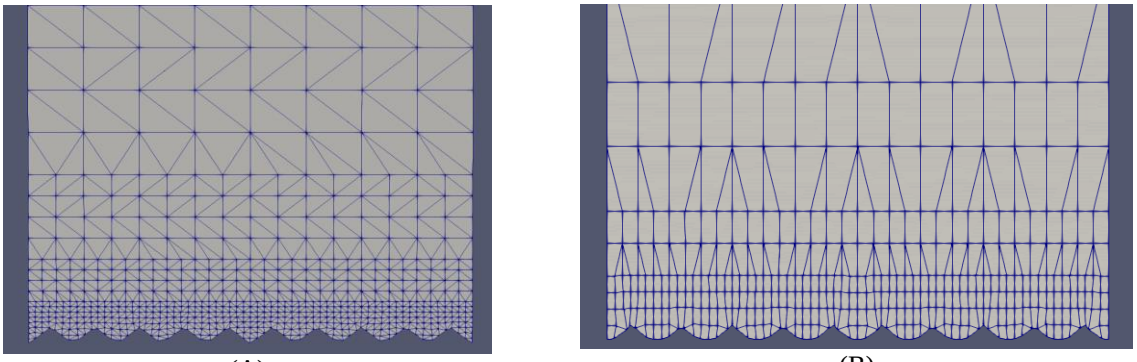

(A) (B)

Fig. 5. Mesh of (A) Sawtooth Riblets and (B) U-Shaped Riblets

Fig. 5 (A) and (B) show the front view of the mesh created around the riblets. The SnappyHexMesh feature allows for localized refinement and snapping refinement which helps capture the shape of the riblets. The meshing process for the riblet geometries is done multiple times such that the shape of the riblets is perfectly captured while maintaining a low number of cells in the far-field region. Optimizing the mesh is a critical part of the simulation as it can help in reducing the time taken for the simulation to finish. Different meshes are tested and, refinement zones are specified very closely such that the number of cells do not increase a lot. The final mesh for the Sawtooth riblets contains 9,785,543 cells and U-shaped riblets contain 9,201,215 cells.

2.2 Solver Settings

The three primary approximating-simulation methods used for fluid flow are Spalart-Allmaras, Reynolds-Averaged Navier Stokes (RANS), and Large Eddy Simulations (LES). Out of these three, LES has been predominantly used for simulating complex compressible flows in nozzles, however, compressible-RANS coupled with fine mesh characteristics can also be used to produce good results. The compressible-RANS equation is also known as the Favre-Averaged Navier-Stokes equation, which can be presented as the following three equations:

$$\frac{\partial \bar{\rho}}{\partial t} + \frac{\partial}{\partial x_j}(\rho \widehat{u_j}) = 0 \qquad \text{(Eq. 1.)}$$

$$\frac{\partial (\bar{\rho}\widehat{u_i})}{\partial t} + \frac{\partial}{\partial x_j}\left(\bar{\rho}\widehat{u_j}\widehat{u_i}\right) = -\frac{\partial p}{\partial x_i} + \frac{\partial \bar{\sigma}_{ij}}{\partial x_j} + \frac{\partial \tau_{ij}}{\partial x_j} \qquad \text{(Eq. 2.)}$$

$$\frac{\partial (\bar{\rho}\widehat{E})}{\partial t} + \frac{\partial}{\partial x_j}\left(\bar{\rho}\widehat{u_j}\widehat{H}\right) = \frac{\partial}{\partial x_i}\left(\bar{\sigma}_{ij}\widehat{u_j} + \overline{\sigma_{ij}u_i''}\right) - \frac{\partial}{\partial x_j}(\bar{q}_j + \overline{c_p \rho u_j'' T''} - \hat{u}_i \tau_{ij} + \frac{1}{2}\rho \overline{u_i'' u_i'' u_j''}) \qquad \text{(Eq. 3.)}$$

This study uses the k-w SST (Shear Stress Transport) model, due to its higher stability under adverse pressure gradients and its advantage in modelling near-wall flow behavior. The rho-SIMPLE solver is used for this simulation. rho-SIMPLE is a compressible pressure-based solver which is used instead of SONIC and PIMPLE foam due to the stability of the simulation. Due to the formation of shock waves in the nozzle, an adjustable-time setting was used to reduce time-steps in order to further stabilize the simulation.

2.3 Grid Dependence

A grid dependence test is performed on the base case to validate the CFD framework. Three versions of the mesh are developed: coarse, fine and very fine. Due to the dimensions of the model, a one-cell increase of the mesh causes a much more drastic increase on the overall cell count. The width of the geometry had to consist of more than 8 cells for snapping to occur successfully when producing the mesh for the riblet geometries.

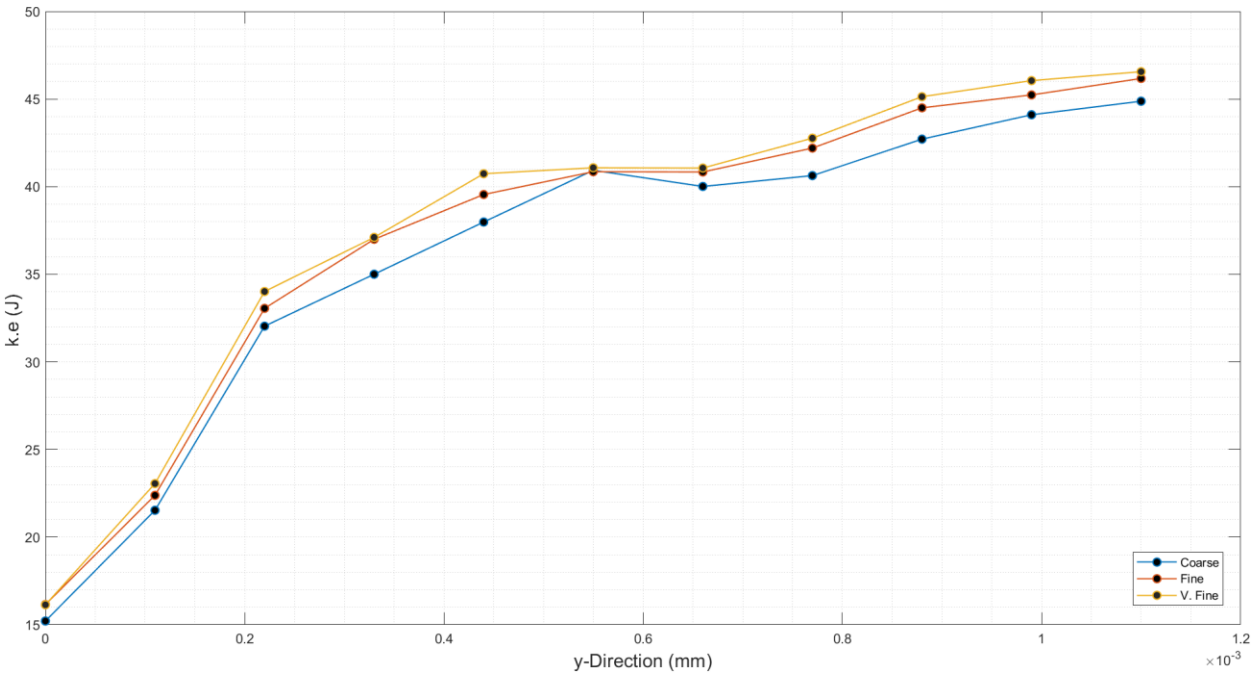

Fig. 6. Kinetic Energy (k.e) v/s Y-Direction

The graph above can be used to show how the results of the simulation are independent of the mesh. Since one of the main focus parameters of this study is the flow in the near wall region, and thus the kinetic energy is taken as a comparing medium. It is evident that the deviation of the graphs is quite low, however, the coarse mesh is not able to properly capture the pattern which is noticed through the fine and very fine meshes. There is very minimal difference in results between the fine and very fine mesh, but the increase in the total number of cells and the time to run the simulation increases substantially. Therefore, the 'fine' mesh is used as a base for all the simulations.

3. Result and Discussion

The study performed by Tsunoda et al. (2000) showed that the effect of adding riblets helps in reducing pressure losses and effectively delays boundary layer separation. Through CFD analysis, this study also shows that the effect of adding riblets in nozzles can improve the flow behavior. Moreover, different geometries of riblets can also be simulated such that the flow around them can be collectively compared. This study focuses on two geometries of riblets, namely, sawtooth and U-shaped.

3.1 Plain Nozzle Surface Case

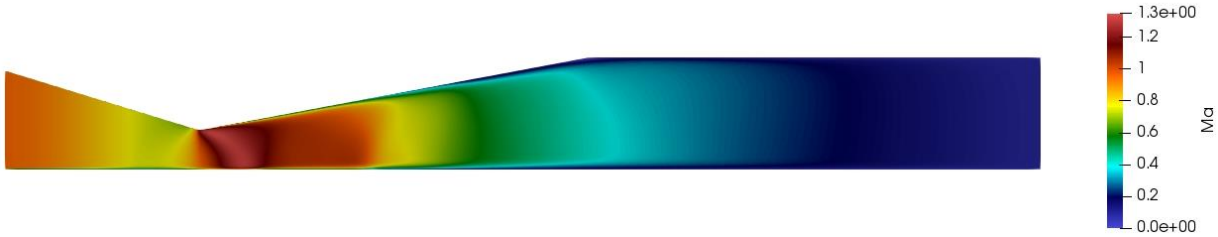

Fig. 7. Velocity Contour of Plane Nozzle Surface Model

Fig. 7 above shows the velocity contours taken from a bisecting plane. The contours clearly show the shock wave production and the boundary layer generation. Boundary layer formation begins around 75mm from the throat and reaches the maximum height at around 100mm from the throat. A similar pattern can be identified in the experimental results of Tsunoda et al. (2000).

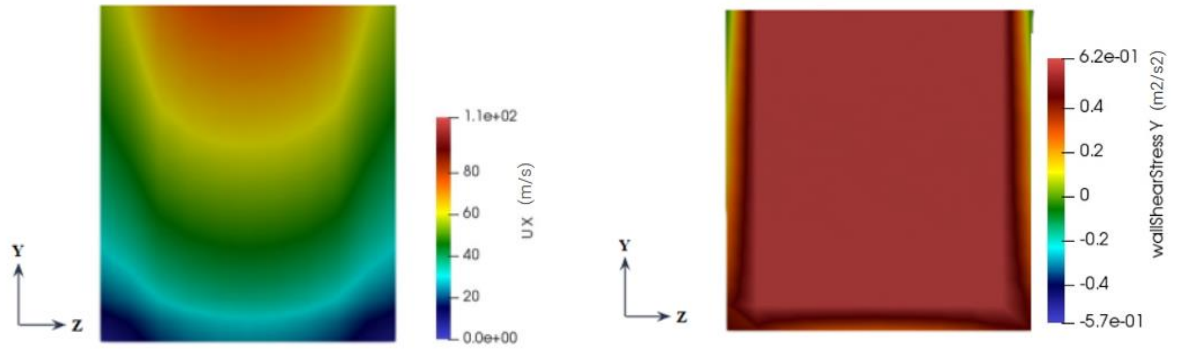

(A) (B)

Fig. 9. (A) Velocity and (B) Wall Shear Stress at Front-Cross Section of Nozzle

Fig. 9 shows the velocity distribution (A) and the wall shear stress (B) in the lower half of the nozzle after the throat. The velocity profiles show the no-slip region and the wall shear stress contours are spread completely over the surface of the nozzle.

Fig. 10. Pressure Contour of Nozzle

Fig. 10 shows the pressure contour of the nozzle. Fig. 11 can be further utilized to analyses the specific fluctuations in pressure to identify the shockwaves and the point of flow separation. The graph shows pressure data over the length of the nozzle at a height of 0.001 m. After the first dip in pressure, a small increase occurs 0.0278 m after the throat, which signifies the shock wave production. However, a second dip and increase pattern are also observed, which signifies the flow separation due to the adverse pressure gradient in the region.

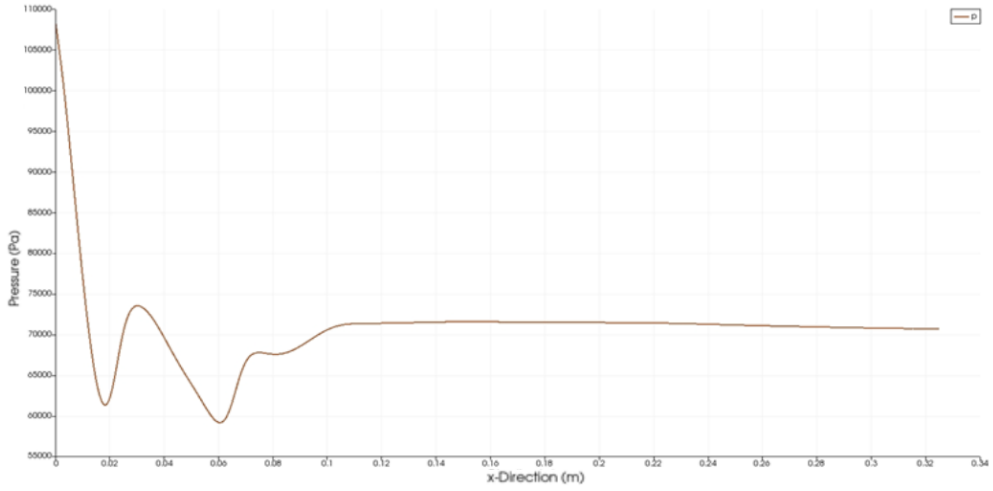

Fig. 11. Pressure v/s X

Kinetic energy can also be used as a method to compare the effect of riblets. Since the induced secondary flows help increase the kinetic energy of the boundary layer flow, the kinetic energy can be plotted from the floor of the nozzle until the flow reaches its free stream velocity.

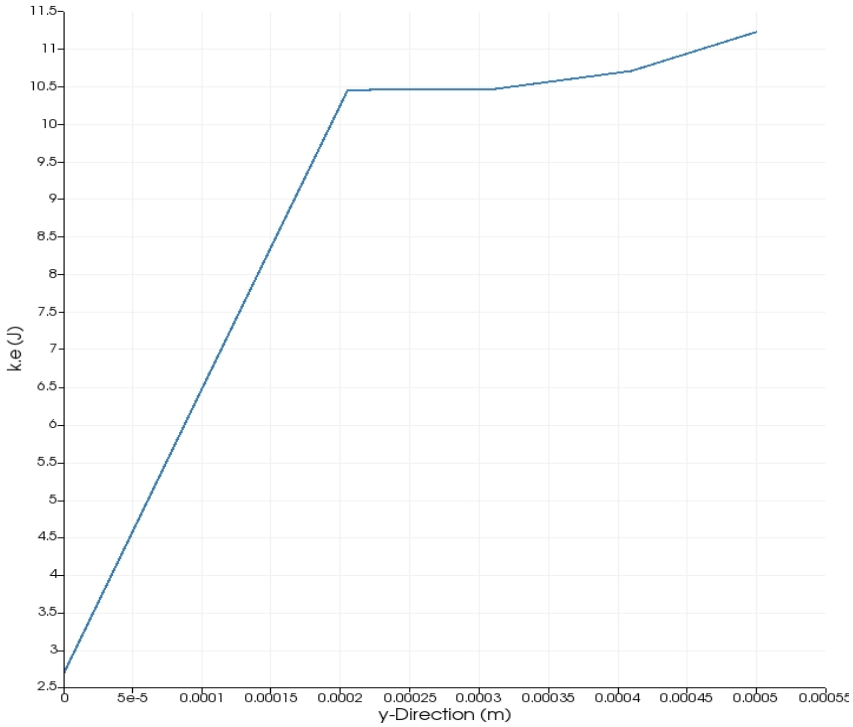

Fig. 12. Kinetic Energy v/s Y

Fig. 12 shows the pattern of the kinetic energy (k.e), as visible, the bare-nozzle has several dips in kinetic energy and this indicates that the near-wall flow is very unsteady. The sharp increase in the energy can be attributed to the interference of free-stream flow on the near-wall region.

3.2 Saw Tooth

The simulations of the sawtooth riblets showed improved flow behavior. The induction of secondary flow in the riblets caused the produced boundary layer to be of a smaller height. The flow was noticed to be more stable along the walls of the nozzle.

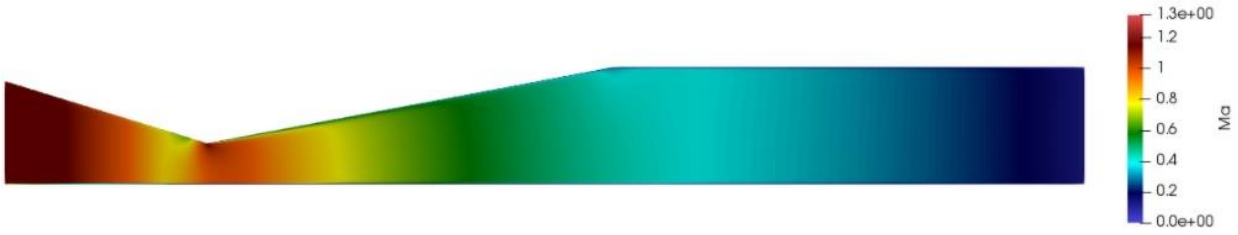

Fig. 13. Velocity Contour (Sawtooth)

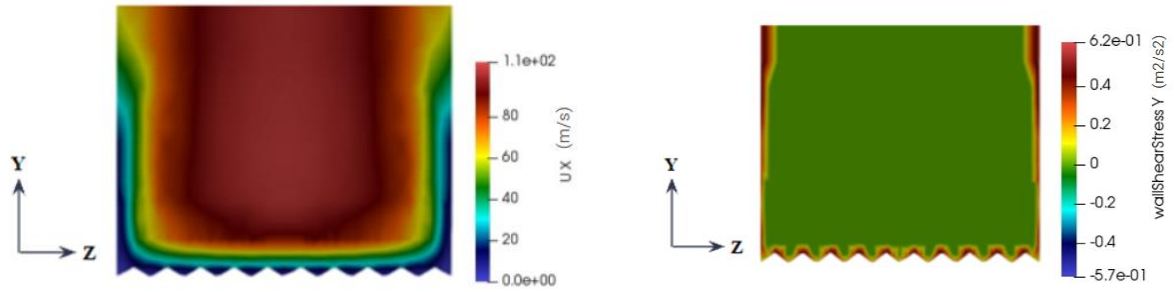

(A) (B)

Fig. 14. (A) Velocity Contour and (B) Wall Shear Stress Around Sawtooth Riblets

Fig. 14 (A) and (B) above depict the velocity contours and the wall shear stress. The velocity contours perfectly show the effect of the riblets. Due to the formation of secondary flows, the pockets of zero velocity flow are created in the riblets and a stable layer of constant velocity can be noticed being developed above the riblets.

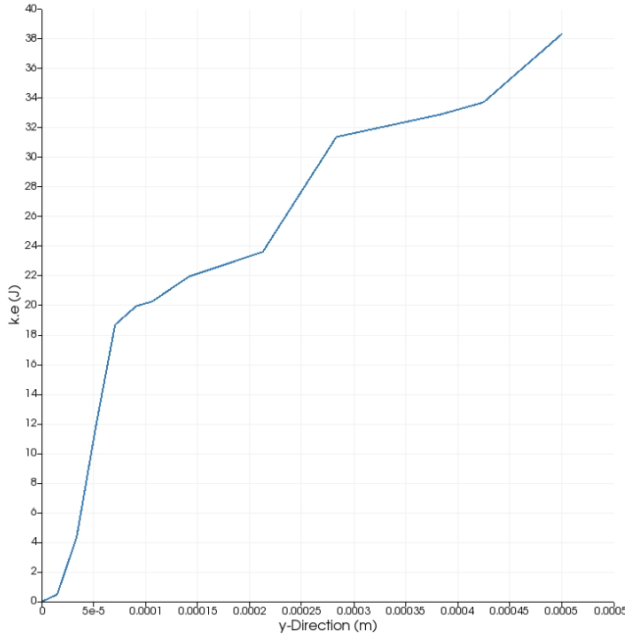

Fig. 15. Kinetic Energy v/s Y (Sawtooth)

The high-speed flow above the riblets has high kinetic energy, this results in delayed flow separation. The graph above shows the kinetic energy against the y-direction. The increasing kinetic energy of the flow as it gets further from the wall also facilitates keeping the boundary layer attached. This is majorly due to the increased momentum of the flow. Furthermore, the secondary flows also induce vortical patterns in the flow, which also aids in adding the high energy free-stream flow into the boundary layer, further enhancing its attachment. Based on the comparisons presented by Tsunoda et al. (2000), another comparison can be discussed based on the average streamwise variation of stagnation pressure.

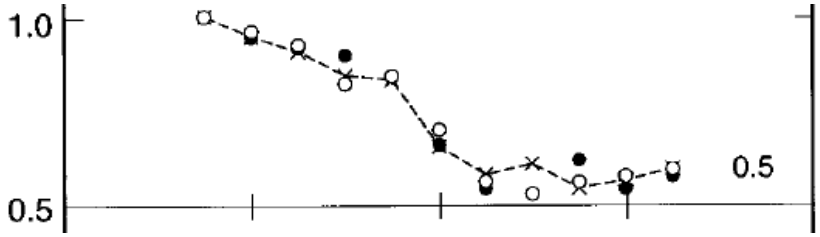

(A)

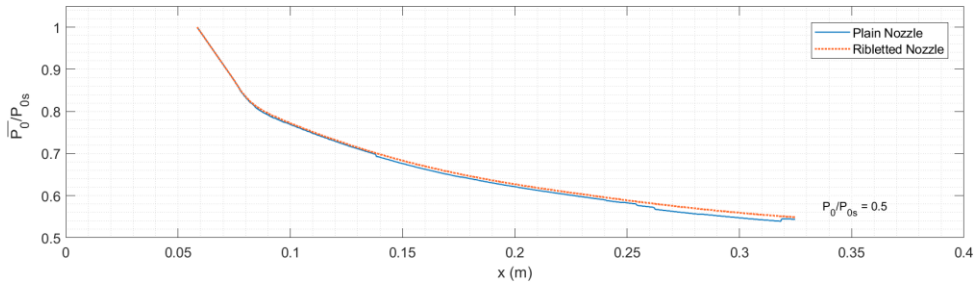

(B)

Fig. 16 Comparison between Experimental (A) and Simulated (B) Pressure Ratios

Fig. 16 can be used to see the similarities in the trend between the experimental and simulated results. Evidently, the pattern of the two graphs is very similar. Experimental results are prone to anomalies and use a limited dataset, whereas the simulated results provide a range of datapoints and provide a smoother graph. Tsunoda et al. (2000) quotes a difference in pressure between the bare and sawtooth-nozzle of 0.10 at a pressure ratio of 0.5, the results from the simulation show a difference of 0.106. The error between the two values is 6% which is particularly reasonable for a RANS model.

3.3 U-Shaped

Fig. 17. Velocity Contour (U-Riblets)

U-shaped riblets were observed to produce better flow characteristics than the sawtooth riblets. The effect of these riblets can be seen in the velocity plot (Fig. 18), where the boundary layer is smaller and the flow is much more stable. Through the contours around the riblets, it is possible to see the differences in flow behavior. Fig. 18 (A) and (B) below give the velocity and the wall shear stress contours, respectively, and it is clear from the contours that the regions of high stress are concentrated even more. The pointed tips of the 'U' are where the stress is concentrated. The localization of stress to small regions helps in reducing the overall damage on the nozzle inner wall.

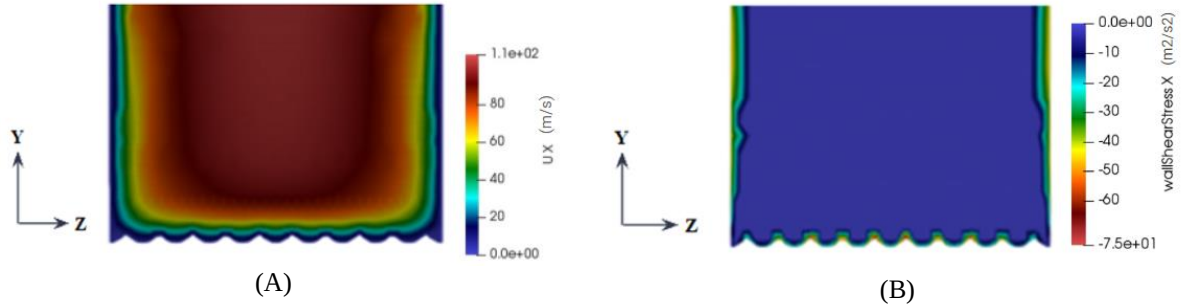

Fig. 18. (A) Velocity Contour and (B) Wall Shear Stress around U- Riblets

Moreover, the kinetic energy (K.E.) versus Y-direction graph can be used to further analyses the boundary layer behavior. As visible, there is a steep increase in K.E, and in comparison, to the sawtooth riblets, the K.E. reaches a higher value, this suggests the higher energy in the near-wall flow and hence, higher momentum. Higher momentum in the boundary layer region is crucial to keep the boundary layer attached.

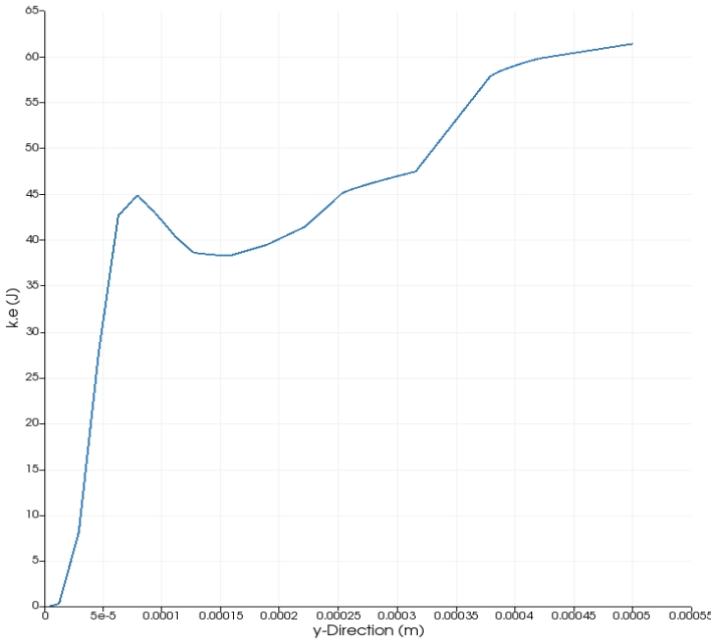

Fig. 19. Kinetic Energy v/s Y (U-Riblets)

4. Conclusion

Simulations are successfully carried out and the CFD framework is optimized with focus on computational load and accuracy of results. The riblets have been shown to produce the expected flow patterns. The low velocity pockets are formed between the riblets and the wall shear stress contours suggest to the localization of stress on the riblet tips which is an expected result. Further comparison is made between the base case, sawtooth riblets and U-shaped riblets though the velocity contours, wall shear stress contours and the kinetic energy of the flow.

- The velocity contours suggest that the pockets of low-speed flow are created between the riblets and the high-speed flow is elevated above the tips of the riblets.
- The elevated high-speed flow, also results in the wall shear stress to be largely concentrated on the tips of the riblets.
    - It is realized that the U-shaped riblets work better in concentrating the high stress to its tips due to the high velocity flow being concentrated above riblets. This helps in reducing lateral loads as well as improves the longevity of the surface.
- By comparing the patterns in the fluctuations of kinetic energy of the flow, it is observed that the base case has the most energy fluctuations, which show the instability in flow. The riblets are able to keep the near-wall flow more stable, however, the U-shaped riblets are more successful in reaching a higher energy under the same distance. Higher energy equates to higher momentum of flow; hence boundary layer separation is delayed.
- Flow is more stable with the addition of the riblets and a small boundary layer forms and sustains itself until the exit.

5. Acknowledgement

The researchers of this study would like to humbly thank the Fluid Mechanics Research Group and the Mechanical Engineering Department in Delhi Technological University for providing us with guidance and the resources to conduct the study.

6. Reference

[1] Johnson, A., & Papamoschou, D., (2010). Instability of shock-induced nozzle flow separation. Physics of Fluids. 2010;22(1):016102.

[2] Smalley, K., Brown, A., Ruf, J., & Gilbert, J., (2007). Flow Separation Side Loads Excitation of Rocket Nozzle FEM. 48th AIAA Conference.
[3] Östlund, J., (2002). low processes in rocket engine nozzles with focus on flow-separation and side-loads. PhD Thesis, Royal Inst of Tech, Stockholm, TRITA-MEK. 2002.
[4] Khobragade, N., Wylie, J., Gustavsson, J., & Kumar, R., (2019). Control of Flow Separation in a Rocket Nozzle Using Microjets. New Space. 2019;7(1):31-42.
[5] Duan L, Choudhari M., (2012). Effects of Riblets on Skin Friction and Heat Transfer in High-Speed Turbulent Boundary Layers. 50th AIAA Aerospace Sciences Meeting including the New Horizons Forum and Aerospace Exposition.
[6] Walsh, M., (1982). Turbulent boundary layer drag reduction using riblets. 20th Aerospace Sciences Meeting. 1982.
[7] Tsunoda, K., Suzuki, T., & Asai, T., (2000). Improvement of the Performance of a Supersonic Nozzle by Riblets. Journal of Fluids Engineering. 2000;122(3):585-591.
[8] Goldstein, D., & Tuan, T., (1998) Secondary flow induced by riblets. Journal of Fluid Mechanics. 1998;363:115-151.
[9] Stark, R., (2013). Flow Separation Side Loads Excitation of Rocket Nozzle FEM. 48th AIAA/ASME/ASCE/AHS/ASC Structures, Structural Dynamics, and Materials Conference. 2007.
[10] Bechert D, Hage W., (2006). Drag reduction with riblets in nature and engineering. Flow Phenomena in Nature Volume 2. 2006;:457-504.
[11] Ghosh, A., Gupta, P., J., & Singh, R. K., (2021). Metaheuristic Optimization Framework for Drag Reduction Using Bioinspired Surface Riblets. arXiv preprint arXiv:2109.09650. 2021.
[12] Lee, S., & Lee, S., (2001). Flow field analysis of a turbulent boundary layer over a riblet surface. Experiments in Fluids. 2001;30(2):153-166.
[13] Martin, S. and Bhushan, B., (2016). Discovery of riblets in a bird beak for low fluid drag. Philosophical Transactions of the Royal Society A: Mathematical, Physical and Engineering Sciences, 374(2073), p.20160134.